

## ADHESION AND CAPILARITY IN MICRO-BEARING LUBRICATION

**Krzysztof Wierzcholski**

*Technical University of Koszalin  
Institute of Mechatronics, Nanotechnology and Vacuum Technique  
Raclawicka Street 15-17, 75-620 Koszalin, Poland  
tel.: +48 505729119, fax: +48 94 3478489  
e-mail: krzysztof.wierzcholski@wp.pl*

**Andrzej Miszczak**

*Maritime University Gdynia, Faculty of Marine Engineering  
Morska Street 81-87, 81-225 Gdynia, Poland  
tel.: +48 58 6901348, fax: +48 58 6901399  
e-mail: miszczak@am.gdynia.pl*

### **Abstract**

*Present paper shows the some main phenomena which have important influence on the micro-bearing operating parameters. To above mentioned phenomena belong: adhesion forces, adsorption forces, capillary forces, elastic and hyperelastic deformations of cooperating micro-bearing surfaces, Van-der Waals electrostatic forces on the micro-bearing surfaces. Because the height of super thin micro-bearing gap is very small often smaller than 1 micrometer, hence the adhesion forces and capillary forces arising in micro-bearing gap, provoke the oil dynamic viscosity changes. This fact leads to the hydrodynamic pressure and bearing carrying capacity changes.*

*The performed research play off the main role of mechanical micro-deformations of cooperating micro-bearing surfaces on non-Newtonian oil dynamic viscosity and here are indicated the influence of capillary force on adhesion forces in micro-scale.*

*The micro-deformations of the micro-bearing gap height are effecting the changes of oil flow velocity in the gap, this fact leads to the share rate changes and therefore we obtain changes of apparent viscosity of the non-Newtonian oil.*

**Keywords:** *adsorption, adhesion, capillary forces, micro-bearing lubrication*

### **1. Introduction**

In recent papers which had been investigated mostly the adhesion phenomena in experimental way [1-11] are not taken into account in analytical way the influences of adhesion forces and capillary forces simultaneously with elastic and hyperelastic micro-bearing gap height deformations on oil viscosity changes and on the micro-bearing operating parameters.

Present paper elaborates the preliminary derivations of basic hydrodynamic equation of lubrication for micro-bearing in the case if during the lubrication the adhesion forces, capillary forces and elastic or hyperelastic deformations of micro-bearing gap height are taking into account.

Here are presented the possibilities to derive the hydrodynamic pressure distributions, load carrying capacity, friction forces and friction coefficients in slide micro-bearings gaps taking into account the adhesion and capillary forces with simultaneously effects of gap height deformations.

The changes of gap height are described by the formula:

$$\varepsilon_T = \varepsilon + \varepsilon_\Delta. \quad (1)$$

We denote:

- $\varepsilon_T$  - total gap height,
- $\varepsilon$  - classical gap height,
- $\varepsilon_\Delta$  - gap height changes caused by elastic or hyperelastic deformations.

We assume that the adhesion forces and capillary forces can to change the dynamic oil viscosity in super thin micro-bearing gap. The changes are described by the following formula:

$$\eta_T(\alpha_1, \alpha_2, \alpha_3) = \eta(\alpha_1, \alpha_3) + \eta_{adh}(\alpha_1, \alpha_2, \alpha_3) + \eta_{cap}(\alpha_1, \alpha_2, \alpha_3). \quad (2)$$

We denote:

- $\eta_T$  - total oil dynamic viscosity,
- $\eta$  - classical oil dynamic viscosity,
- $\eta_{adh}$  - oil dynamic viscosity caused by the adhesion forces,
- $\eta_{cap}$  - oil dynamic viscosity caused by the capillary forces.

Molecules of the oil can be adsorbed on a cooperating micro-bearing surfaces and create high elasticity layer. Capillary and adhesion forces change the dynamic oil viscosity if gap height is smaller then 1 micrometer. Fig. 1 show the some factors which have influence on the micro-bearing lubrications. Of course, here is indicated adhesion and capillary phenomenon.

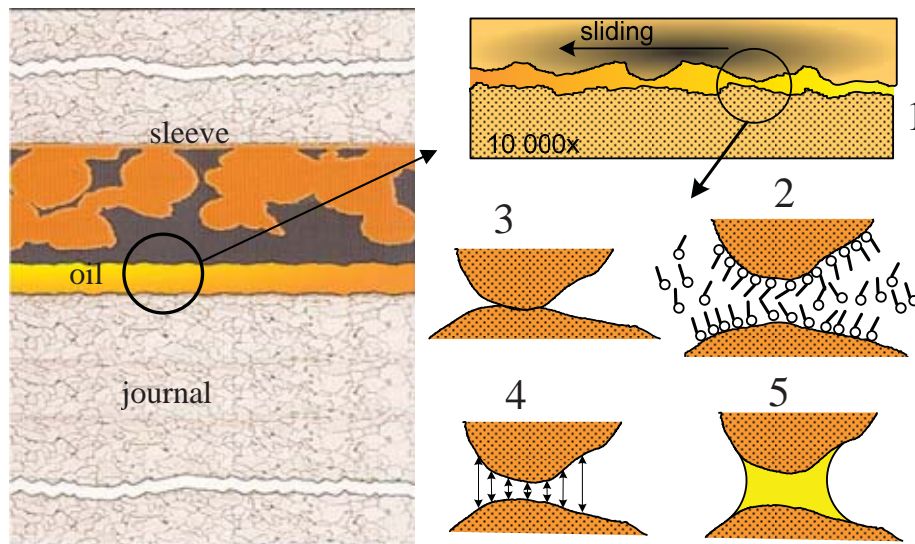


Fig. 1. Main factors which have influence on hydrodynamic lubrication of micro-bearings: 1 – nano roughness of surfaces, 2 – adsorption layers, 3 – elastic and hyperelastic deformations of surfaces, 4 – Van der Waals electrostatic forces, 5 – capillary forces

Figure 2 illustrates the changed length  $a$  of the contact gap in micro-bearings in two cases namely: if compressive and tensile forces act in contact region and if only compressive elastic forces in region of the contact arise. In above mentioned two cases we have respectively:

$$l^3 = \frac{R}{K} (P + 3\pi Rq + \sqrt{6\pi RqP + (3\pi Rq)^2}), \quad (3)$$

$$l^3 = \frac{3PR}{4E^*} \quad P = P_{adh} + P_0, \quad (4)$$

where:

- $l$  - length of the contact in m,
- $K$  - bulk elasticity modulus in  $N/m^2$ ,

R - radius of the journal in m,  
 P - force in N,  
 q - load on the length unit in N/m,  
 $P_{adh}$  - adhesion force in N.

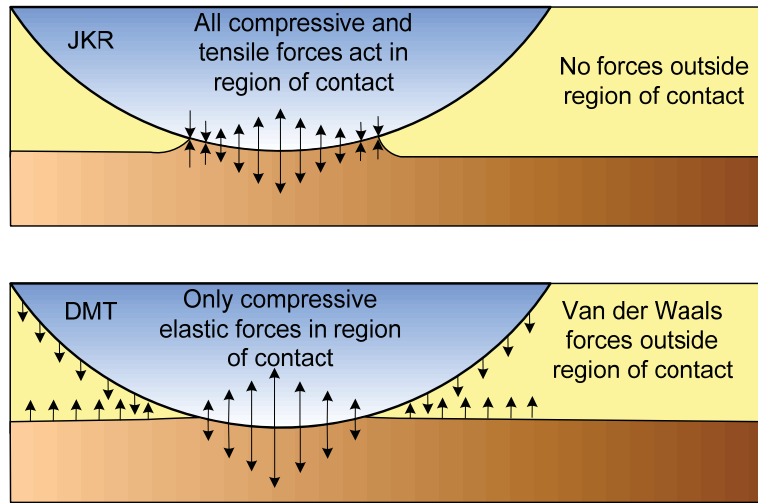


Fig. 2. Two cases of adhesion contact of elastic bodies

Figure 3 illustrates the parabolic journal of HDD micro-bearing. The groove and ridge geometry located on the parabolic surface are presented in Fig. 3. The grooves can be situated in circumferential or longitudinal directions [2]. Groove location affects the dynamic performance of HDD spindle system.

The micro-bearing lubrication is characterized by the dynamic viscosity changes in thin gap- height direction.

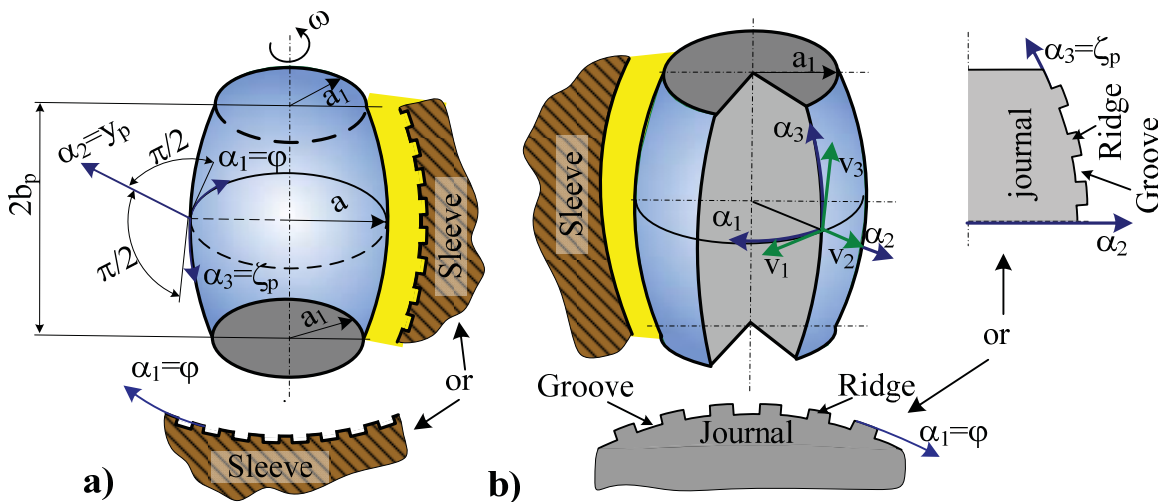


Fig. 3. Parabolic journal for hydrodynamic HDD micro-bearing (20 000 rpm after K. Wierzcholski): a) circumferential or longitudinal grooves on the parabolic sleeve, b) longitudinal or circumferential grooves on the parabolic journal

## 2. Pressure distributions in curvilinear micro-bearings gaps

For the parabolic micro-bearing we assume following co-ordinates:  $\alpha_1 = \varphi$ ,  $\alpha_2 = y_p$ ,  $\alpha_3 = \zeta_p$ . Mentioned coordinates are presented in Fig. 3. For parabolic journal we have:  $a_1$  – the smallest radius of the hyperbolic journal,  $a$  – the largest radius of the hyperbolic journal,  $2b_p$  – the bearing length

(see Fig. 3). From the system of conservation of momentum and continuity equation after thin boundary layer simplifications and boundary conditions in the curvilinear coordinates  $(\alpha_1, \alpha_2, \alpha_3)$  we obtain the dimensional pressure function  $p(\alpha_1, \alpha_3, t)$  satisfying the modified Reynolds equations in the following curvilinear form [6]:

$$\begin{aligned} \frac{\partial}{\partial \alpha_1} \left[ \left( \frac{\partial E(p)}{\partial \alpha_1} + \frac{\partial E(p_{adh})}{\partial \alpha_1} + \frac{\partial E(p_{cap})}{\partial \alpha_1} \right) E \left( \int_0^{\varepsilon_T} A_\eta d\alpha_2 \right) \right] + \frac{h_1}{h_3} \frac{\partial}{\partial \alpha_3} \left[ \frac{h_1}{h_3} \left( \frac{\partial E(p)}{\partial \alpha_3} + \right. \right. \\ \left. \left. + \frac{\partial E(p_{cap})}{\partial \alpha_3} \right) E \left( \int_0^{\varepsilon_T} A_\eta d\alpha_2 \right) \right] = \omega h_1^2 \frac{\partial}{\partial \varphi} \left[ E \left( \int_0^{\varepsilon_T} A_s d\alpha_2 \right) - E(\varepsilon_T) \right] + h_1^2 \left[ \frac{\partial E(\varepsilon)}{\partial t} + \frac{\partial E(\varepsilon_\Delta)}{\partial t} \right], \end{aligned} \quad (5)$$

where:

$E$  - denotes expectancy function,

$\varepsilon_T(\alpha_1, \alpha_3, t)$  - total gap height,

$p_{adh}$  - changes of pressure caused by the adhesion,

$p_{cap}$  - changes of pressure caused by the capillary forces.

Flow is generated by journal rotation and the sleeve is motionless. Lubricant velocity components  $v_1, v_2, v_3$  in  $\alpha_1, \alpha_2, \alpha_3$  directions, respectively, have the following form [6]:

$$v_1(\alpha_1, \alpha_2, \alpha_3, t) = \frac{1}{h_1} \left( \frac{\partial p}{\partial \alpha_1} + \frac{\partial p_{adh}}{\partial \alpha_1} + \frac{\partial p_{cap}}{\partial \alpha_1} \right) A_\eta + (1 - A_s) \omega h_1, \quad (6)$$

$$v_3(\alpha_1, \alpha_2, \alpha_3, t) = \frac{1}{h_3} \left( \frac{\partial p}{\partial \alpha_3} + \frac{\partial p_{adh}}{\partial \alpha_3} + \frac{\partial p_{cap}}{\partial \alpha_3} \right) A_\eta, \quad (7)$$

$$v_2(\alpha_1, \alpha_2, \alpha_3, t) = - \int_0^{\alpha_2} \frac{1}{h_1} \frac{\partial v_1}{\partial \alpha_1} d\alpha_2 - \int_0^{\alpha_2} \frac{1}{h_1 h_3} \frac{\partial (h_1 v_3)}{\partial \alpha_3} d\alpha_2 \quad (8)$$

and

$$A_s(\alpha_1, \alpha_2, \alpha_3, t) \equiv \frac{\int_0^{\alpha_2} \frac{1}{\eta + \eta_{adh} + \eta_{cap}} d\alpha_2}{\int_0^{\varepsilon_T} \frac{1}{\eta + \eta_{adh} + \eta_{cap}} d\alpha_2},$$

$$A_\eta(\alpha_1, \alpha_2, \alpha_3, t) \equiv \int_0^{\alpha_2} \frac{\alpha_2}{\eta + \eta_{adh} + \eta_{cap}} d\alpha_2 - A_s(\alpha_1, \alpha_2, \alpha_3, t) \int_0^{\varepsilon+\varepsilon_\Delta} \frac{\alpha_2}{\eta + \eta_{adh} + \eta_{cap}} d\alpha_2, \quad (9)$$

where:

$\eta = \eta(\alpha_1, \alpha_3)$  - liquid dynamic viscosity,

$t$  - time,

$0 \leq \alpha_2 \leq \varepsilon_T, 0 \leq \alpha_1 < 2\pi\theta_1, 0 \leq \theta_1 < 1$  and  $-b_p \leq \alpha_3 \leq b_p$  for parabolic journal.

For the parabolic shapes of micro-bearing journals we have following coordinates:  $\alpha_1 = \varphi$ ,  $\alpha_2 = y_p$ ,  $\alpha_3 = \zeta_p$ , and Lamé coefficients are as follows:

$$h_1 = a \cos^2(\Lambda_{p1} \zeta_{p1}), \quad h_3 = \sqrt{1 + 4(\Lambda_{p1}/L_{p1})^2 \sin^2(\Lambda_{p1} \zeta_{p1})} \cos(\Lambda_{p1} \zeta_{p1}), \quad (10)$$

$$|\zeta_{p1}| \leq \frac{1}{\Lambda_{p1}} \arccos \sqrt{\frac{a_1}{a}}, \quad \Lambda_{p1} \equiv \sqrt{\frac{a - a_1}{a}}, \quad L_{p1} \equiv \frac{b_p}{a},$$

where  $a$ ,  $a_1$ ,  $b_h$  are defined before.

### 3. Friction forces in curvilinear micro-bearing gap

This section presents the friction forces calculation in curvilinear micro-bearing gaps. The components of friction forces in curvilinear  $\alpha_1$ ,  $\alpha_3$  directions occurring in micro-bearing gaps have the following forms:

$$F_{R1} = \iint_F \left[ (\eta + \eta_{adh} + \eta_{cap}) \frac{\partial v_1}{\partial \alpha_2} \right]_{\alpha_2 = \varepsilon_T} h_1 h_3 d\alpha_1 d\alpha_3, \quad (11)$$

$$F_{R3} = \iint_F \left[ (\eta + \eta_{adh} + \eta_{cap}) \frac{\partial v_3}{\partial \alpha_2} \right]_{\alpha_2 = \varepsilon_T} h_1 h_3 d\alpha_1 d\alpha_3,$$

where:

$\eta = \eta(\alpha_1, \alpha_3)$  - liquid dynamic viscosity,

$t$  - time,

$F$  - lubrication surface,

$v_1, v_3$  - fluid velocity components (6), (7) in  $\alpha_1$ ,  $\alpha_3$  directions,

$h_1, h_3$  - Lamé coefficients (10) in  $\alpha_1$ ,  $\alpha_3$  directions.

Putting formulae (6), (7) into equation (11) for curvilinear journal, then we obtain the friction components  $F_{R1}$ ,  $F_{R3}$  in circumferential  $\alpha_1$ , and longitudinal  $\alpha_3$  directions, respectively:

$$F_{R1} \equiv F_{R\varphi} = \iint_F \left[ \frac{\eta + \eta_{adh} + \eta_{cap}}{h_1} \left( \frac{\partial p}{\partial \alpha_3} + \frac{\partial p_{adh}}{\partial \alpha_3} + \frac{\partial p_{cap}}{\partial \alpha_3} \right) \frac{\partial A_\eta(\alpha_1, \alpha_2, \alpha_3)}{\partial \alpha_2} \right]_{\alpha_2 = \varepsilon_T} h_1 h_3 d\alpha_1 d\alpha_3 +$$

$$- \iint_F \left[ \omega h_1 (\eta + \eta_{adh} + \eta_{cap}) \frac{\partial A_s(\alpha_1, \alpha_2, \alpha_3)}{\partial \alpha_2} \right]_{\alpha_2 = \varepsilon_T} h_1 h_3 d\alpha_1 d\alpha_3, \quad (12)$$

$$F_{R3} = \iint_F \left[ \frac{\eta + \eta_{adh} + \eta_{cap}}{h_3} \left( \frac{\partial p}{\partial \alpha_3} + \frac{\partial p_{adh}}{\partial \alpha_3} \right) \frac{\partial A_\eta(\alpha_1, \alpha_2, \alpha_3)}{\partial \alpha_2} \right]_{\alpha_2 = \varepsilon_T} h_1 h_3 d\alpha_1 d\alpha_3, \quad (13)$$

where for parabolic journal we have  $F_{R3} \equiv F_{R\zeta_p}$ .

Friction coefficients of parabolic micro-bearing journals are as follows:

$$\mu_p = \frac{\sqrt{(F_{R\varphi})^2 + (F_{R\zeta_p})^2}}{C_{tot}^{(p)}}, \quad (14)$$

where  $C_{tot}^{(p)}$  is the load carrying capacity in parabolic coordinates.

#### 4. Numerical calculations

The pressure distributions and capacity values in machine parabolic slide micro-bearings ( $\alpha_1 \equiv \varphi$ ,  $\alpha_2 \equiv y_p$ ,  $\alpha_3 \equiv \zeta_p$ ) are determined in the lubrication region  $\Omega_c$ , which is defined by the following inequalities:  $0 \leq \varphi \leq \varphi_k$ ,  $-b_p \leq \zeta_p \leq b_p$  where  $2b_p$  – micro-bearing length.

Numerical calculations are performed in Mathcad 14 Professional Program by virtue of the equation (2) by means of the finite difference method (see Fig. 4 and 5).

The gap height of the parabolic micro-bearing and bio-bearing has the following form:

$$\varepsilon_T = \varepsilon(1 + \lambda_p \cos \varphi), \quad (15)$$

where:

$\lambda_p$  - eccentricity ratio in parabolic micro-bearing,

$\varepsilon$  - radial clearance of parabolic micro-bearing.

Oil dynamic viscosity is a sum of classical viscosity and viscosity caused by adhesion and cohesion forces what is presented below:

$$\begin{aligned} \eta_T(\varphi, y_p, \zeta_p) &= \eta(\varphi, \zeta_p) + \eta_{akh}(\varphi, y_p, \zeta_p), \\ \eta_{akh}(\varphi, y_p, \zeta_p) &= a_\eta k + b_\eta \left\{ e^{c_\eta [\max(\varepsilon_T) - y_p]} + d_\eta e^{c_\eta [y_p - \max(\varepsilon_T)]} \right\}, \\ a_\eta &= a_{\eta\eta} \cdot \eta, \quad b_\eta = b_{\eta\eta} \cdot \eta, \end{aligned} \quad (16)$$

where:

$k$  - surface curvature,

$a_{\eta\eta}, b_{\eta\eta}, c_\eta, d_\eta$  - experimental coefficients.

Figure 4 and 5 shows the numerical pressure values in parabolic micro-bearing gap for stationary flow without stochastic changes with: largest value of the parabolic journal radius  $a = 0.001$  m, least value of the parabolic journal radius  $a_1 = 0.0008$  m, relative radial clearance  $\psi = 0.002$ , radial clearance  $\varepsilon = 2 \cdot 10^{-6}$  m, dimensionless bearing length  $L_{c1} = b_c/a = 1$ , oil dynamic viscosity  $\eta = 0.030$  Pas, surface curvature  $k = 1000$  m<sup>-1</sup>, experimental coefficients  $a_{\eta\eta} = 0.00004$  m,  $b_{\eta\eta} = 0.0025$ ,  $c_\eta = 3.5/\varepsilon$  m<sup>-1</sup>,  $d_\eta = 181.82$ , angular velocity  $\omega = 754$  s<sup>-1</sup>, characteristic dimension value of hydrodynamic pressure  $p_o = \omega\eta R^2/\varepsilon^2$ ,  $p_o = 5.655$  MPa, relative eccentricity values  $\lambda_c = 0.4$ ,  $\lambda_c = 0.5$ .

By virtue of the boundary Reynolds conditions the angular coordinate of the film end has the values:  $\varphi_k = 3.705$  rad;  $\varphi_k = 3.670$  rad.

If eccentricity ratio increases from  $\lambda_c = 0.4$  to  $\lambda_c = 0.5$ , then the maximum value of hydrodynamic pressure increases from 7.61 MPa to 15.58 MPa and total capacity in  $y_p$  direction increases from 13.64 N to 25.87 N.

Figures 4a and 5a show hydrodynamic pressure distributions inside parabolic micro-bearing gap lubricated by classical Newtonian lubricant for constant dynamic viscosity in gap height direction without changes caused by the adhesion and cohesion.

Figures 4b and 5b show hydrodynamic pressure distributions inside parabolic micro-bearing gap lubricated by classical Newtonian lubricant for variable dynamic in gap height direction caused by the adhesion and cohesion.

#### 5. Conclusions

1. Friction force increases nearly linearly with the normal load but only in case if angular velocity of the journal is very small i.e. journal is motionless and if nano-level of friction forces is not taken into account.

$a = 0.001$  [m],  $a_1 = 0.0008$  [m],  $L_{p1}=b_p/a=1$ ,  $\eta = 0.030$  [Pas],  $\omega=754$  [1/s],  $p_o=5.655$  [MPa]

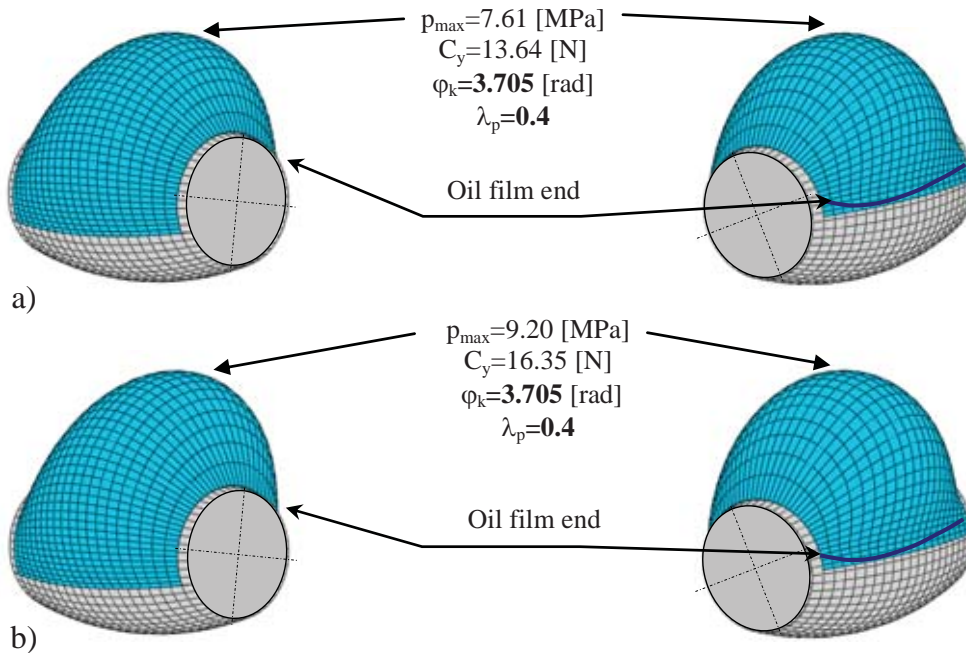


Fig. 4. The pressure distributions in parabolic micro-bearings caused by the rotation in circumferential direction. Left side presents the view from the film origin, right side shows the view from film end: a) without influences of adhesion forces on the oil viscosity, b) with viscosity changes caused by the adhesion

$a = 0.001$  [m],  $a_1 = 0.0008$  [m],  $L_{p1}=b_p/a=1$ ,  $\eta = 0.030$  [Pas],  $\omega=754$  [1/s],  $p_o=5.655$  [MPa]

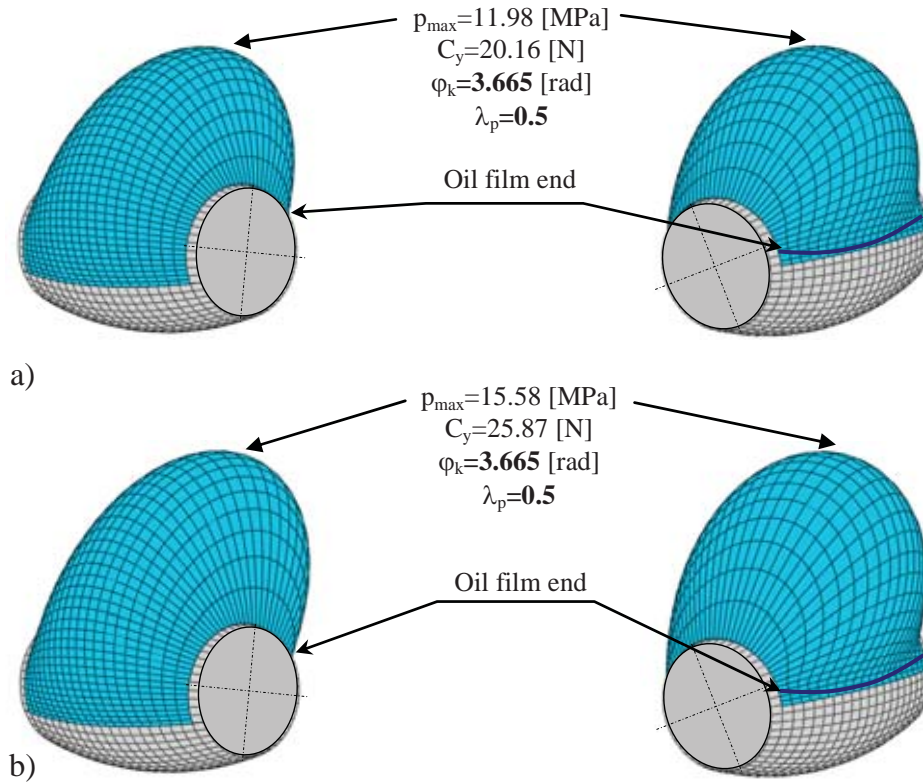


Fig. 5. The pressure distributions in parabolic micro-bearings caused by the rotation in circumferential direction. Left side presents the view from the film origin, right side shows the view from film end: a) without influences of adhesion forces on the oil viscosity, b) with viscosity changes caused by the adhesion

2. Friction force caused by the capillary forces i.e. capillary pressure exists even when the applied normal load is zero and journal is motionless and adhesion forces are neglected
3. Friction forces caused by the journal rotation existed if normal load is zero, adhesion and capillary forces are neglected.
4. Load carrying capacity increases implied by the oil dynamic viscosity increases caused by the adhesion and cohesion forces attain about from 19% to 28% in comparison to the viscosity and capacity values in classical form.

## References

- [1] Taylor, C. J., Dieker, L. E., Miller, K. T., Koh, C. A., Dendy, S. E., *Micromechanical adhesion force measurements between tetrahydrofuran hydrate particles*, Journal of Colloid and Interface Science, Vol. 306, pp. 255-261, 2007.
- [2] Yoon E. S., Yang S. H., Han H. G., Kong H., *An experimental study on the adhesion at a nano-contact*, Wear, Vol. 254, pp. 974-980, 2003.
- [3] De La Fuente, L., Montanes, E., Yizhi M., Yaxin L., Burr, T. J., Hoch, H. C., Mingming, W., *Assessing adhesion force of Type I and Type IV Pili of Xylella fastidiosa bacteria by use of microfluidic flow chamber*, Applied and Environmental Microbiology, Vol. 73, pp. 2690-2696, 2007.
- [4] Kogut, L., Etsion, I., *Adhesion in elastic-plastic spherical microcontact*, Journal of Colloid and Interface Science, Vol. 261, pp. 372-378, 2003.
- [5] Xu, L. C., Logan, B. E., *Adhesion forces functionalized latex microspheres and protein-coated surfaces evaluated using colloid probe atomic force microscopy*, Colloid and Surfaces B, Vol. 48, pp. 84-94, 2006.
- [6] Takeuchi, M., *Adhesion Forces of Charged Particles*, Chemical Engineering Science, Vol. 61, pp. 2279-2289, 2006.
- [7] Miranda, J. A., Oliveira, R. M., *Adhesion phenomena in ferrofluids*, Physical Review E, Vol. 70, pp. 1-11, 2004.
- [8] Rymuza, Z., Kusznierevich, Z., Solarski, T., Kwacz, M., Chizhik, S., Goldade, A. V., *Static friction and adhesion in polimer-polymer micro-bearings*, Wear, Vol. 238, pp. 56-69, 2000.
- [9] Schwender, N., Huber, K., Marravi, F. Al., Hannig, M., Ziegler, Ch., *Initial bioadhesion on surfaces in the oral cavity investigated by scanning force microscopy*, Applied Surface Science, Vol. 252, pp. 117-122, 2005.
- [10] Tsukada, M., Irie, R., Yonemochi, Y., Nada, R., Kamiya, H., Watanabe, W., Kauppinen, E. I., *Adhesion force measurement of a DPI size pharmaceutical particle by colloid probe atomic force microscopy*, Powder Technology, Vol. 141, pp. 262-269, 2004.
- [11] Hongben, Z., Goetzinger, M., Peukert, W., *The influence of particle charge and roughness on particle-substrate adhesion*, Powder Technology, Vols. 135-136, pp. 82-91, 2003.